FREE SURFACE MENISCI ON NARROW HORIZONTAL SURFACES

P.J. Erens* A.A. Dreyer†

(First received April 1995; Final version August 1995)

Abstract

The thickness of liquid films on horizontal surfaces is important in condensation applications and in cooling tower splash-packs. In condensation the heat transfer rate is governed by the thickness of the film covering the cold surface, while in cooling tower splash-packs the volume of liquid splashing and the splash drop sizes formed by the impact of large drops on a slat is a strong function of the thickness of the water film on the slat. The splash volumes and splash drop size influence the thermal performance of splash-packing material. Approximate theoretical models for the calculation of the free surface film profile on finite-width horizontal surfaces with low liquid flow rates are presented. Experimental measurements yielded good agreement between experiment and theory. It is concluded that slat width, surface tension, surface wetting, and edge radii govern the free surface film profiles for low liquid flow rate over sharp edges.

Nomenclature

a, b	Constants defined in equation (7)
C	Constant defined in equation (2), [-]
g	Gravitational acceleration, [m/s^2]
h	Depth of water layer, [m/s^2]
M_l	Liquid mass flux normal to slat, [kg/m^{2}s]
P	Pressure, [Pa]
R	Radius of curvature, [m]
u	Velocity, [m/s]
W	Width of the slat, [m]
x	Distance from centreline of a slat, [m]
y	Vertical position above solid surface, [m]
ϕ	Solid edge angle, [°]
Γ	Flow rate per unit length, [kg/ms]
μ	Dynamic viscosity, [kg/ms]
θ	Contact angle at edge, [°]
θ_c	Equilibrium (or thermodynamic) contact angle on horizontal surface, [°]
ρ	Density, [kg/m^3]
σ	Surface tension, [N/m]

Subscripts

atm	Atmospheric
c	Centreline
d	Dynamic
g	Gas
l	Liquid
s	Static
∞	Far upstream from edge

*Department of Mechanical Engineering, University of Stellenbosch, Stellenbosch, 7600 South Africa

†Department of Mechanical Engineering, University of Stellenbosch, Stellenbosch, 7600 South Africa

Introduction

In the case of condensation of vapour on a horizontal surface, the thickness of the condensate film is of major importance since the film thickness governs the rate of condensation. Current models to predict the condensation rates on horizontal surfaces usually ignore the effect of surface tension on the film thickness (see Leppert & Nimmo [1]; Bejan [2]).

Direct contact cooling towers usually contain packing material to increase the contact area between the water and the air. Splash packing material consisting of horizontal layers of wooden, metal or plastic grids, is often used in large natural draft cooling towers. Water sprayed from above strikes the grids, breaking the incoming drops into smaller and slower drops. The slats of a splash grid are covered by thin films of water which are continuously being fed by small or slow moving drops falling from above which do not remove any of the existing water on the grid. Larger drops, travelling at higher velocities, tend to splash on impact with the slats, removing some of the water on the slat. The time-averaged film thickness is governed by the relative rates of water removal and addition as well as by the geometry (width, edge sharpness, etc.) of the slat. The volume of water removed from the slat and the size distribution of the splash drops formed by an impacting drop are dependent amongst other factors on the thickness of the water film on the slat. The thermal performance of a splash pack can be linked directly to the splash volumes and splash drop size distributions. To study the splashing of water drops on slats covered by thin water films, it

is necessary to have a better understanding of the factors governing the shape of the meniscus present on the upper surface of a horizontal, two-dimensional surface (narrow slat).

Surface tension effects are normally neglected in the theoretical modelling of free surface flows. In many cases the surface tension effects are indeed negligible, e.g. the flow of water over a weir (at high liquid flow rates) or laminar (non-wavy) flow of a thin film down a vertical wall. However, in some cases the surface tension effects are very important in governing the flow of liquid, e.g. in coating flows (see Probstein [3]) and in the 'damming' effect observed when liquid tends to form a thick film near the sharp edge of a horizontal surface.

This study concentrated on the flow of a wetting liquid over sharp (90°) edges of horizontal surfaces. Approximate theoretical models were derived to describe the shape of the free surface on these surfaces. Certain boundary conditions required by the theoretical models were obtained experimentally. The effects of the width of the surface and the liquid flow rate on the film profile were also investigated.

Literature study

Slocum [4] correlated experimentally determined flow profiles for liquid flow over sharp weirs. The final correlation, which did not include a surface tension term, predicted all the data well except for that of the flow of water (which has a high surface tension) flowing over a very low weir (0.208 mm high) at low flow rates ($\Gamma = 9.04$ g/ms).

A simple theoretical model, ignoring surface tension, was proposed by Nedderman [5] to predict the experimental data of Goodridge and Gartside [6] for free surface liquid flow down nearly horizontal surfaces. The model predicts the experimental data well, implying that the surface tension effects are relatively small for the range of flow rates studied.

Leppert and Nimmo [1] and Bejan [2] ignored surface tension in the calculation of the thickness of condensate films on horizontal, double-edged surfaces. Leppert and Nimmo's approximate analytical solution for the average condensation Nusselt number is in good agreement with the numerical solution of Bejan.

Nimmo [7] studied the free surface flow of liquid on a horizontal surface draining off a curved surface, but ignored the effect of surface tension since fairly large curvatures were assumed.

The rising height of liquid above the rim of an overflowing cylinder was determined numerically by Berginck-Martens *et al.*[8] Their mathematical model is in good agreement with their experimental measurements. Their results show that surface tension effects were important for water flowing over the sharp edge at all mass flow rates below 200 g/ms.

Ishimi *et al.* [9] analytically solved the governing equations for the shape of a static meniscus near a single edge. According to their analysis the static film thickness far from the edge of the surface is given by

$$h_{s\infty} = \left[\frac{2\sigma(1-\cos\theta)}{\rho_l g}\right]^{0.5} \qquad (1)$$

where θ is the angle the meniscus makes with the horizontal plane at the edge of the meniscus. Assuming a zero free surface flow velocity along the surface far from the edge, Ishimi *et al.* derived the following approximation for the dynamic meniscus far from the edge

$$h_{d\infty} = h_{s\infty} + \left[\frac{3C(\Gamma/\rho_l)}{2(2g)^{0.5}}\right]^{2/3} \qquad (2)$$

Ishimi *et al.* [9] found that equation (2) predicted their experimental data well with $C = 1.61$.

Hartland and Hartley [10] derived analytical relations to describe the static shapes of various pendant and sessile drops, as well as the static meniscus formed by a liquid film on a long two-dimensional surface.

Mathematical modelling

Consider a long, horizontal surface of width, W, with liquid supplied from the middle of the surface as shown in Figure 1. Two different cases were modelled. In the first case the liquid is continually being supplied to the film at a fixed flow rate. Alternatively, in the static case, the liquid is supplied (at a low flow rate) to the surface only to the point where the liquid is about to overflow over the edges, at which time the liquid supply is terminated.

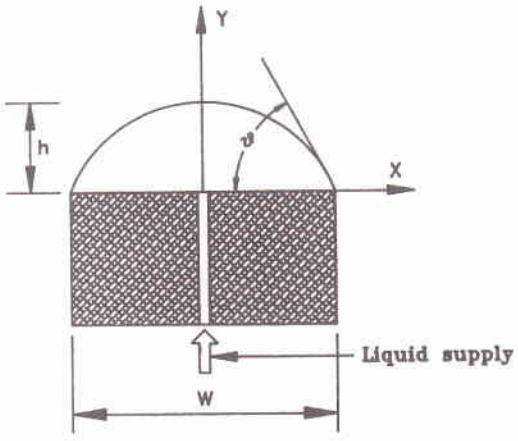


Figure 1 Layout of a typical slat

(a) Solution with non-zero liquid flow rate, $\Gamma > 0$, (dynamic solution)

It is assumed that: (i) the surface is infinitely long, (ii) that the momentum effects are negligible, (iii) the liquid density is much larger than that of the gas phase, and (iv) the liquid flow rate is low. Assumptions (ii) and (iv) imply that the film thickness at the edge of the surface is very thin and that the liquid follows the surface around corner without the formation of a detachment bubble.

Treating the thin liquid film in Figure 1 as a boundary layer, the Navier-Stokes equation in the x direction is

$$-\frac{dP}{dx}+\mu_l\frac{d^2u}{dy^2}=0 \tag{3}$$

The pressure at any position in the film can be expressed as

$$P=P_{atm}+\rho_l g\,(h-y)-\frac{\sigma h''}{\left(1+(h')^2\right)^{3/2}} \tag{4}$$

The third term on the right hand side of equation (4) represents the surface tension term, σ/R. In certain cases where small or gradual changes in the film thickness can be expected this term can be simplified to $\sigma h''$.

Integration of equation (3) with the boundary conditions, $u=0$ at $y=0$ and $(du/dy)=0$ at $y=h$, yields the following expression for the flow velocity in the x-direction

$$u=\frac{1}{u_l}\frac{dP}{dx}\left(0.5y^2-hy\right) \tag{5}$$

From the definition of Γ as mass flow rate per unit length and equation (5) it follows that

$$\Gamma=\rho_l\int_0^h u\,dy=-\frac{\rho_l h^3}{3u_l}\frac{dP}{dx} \tag{6}$$

The flow rate per unit length can be constant or it can vary along the width of the surface as would be the case in condensation. In the case of a constant mass flux normal to the surface it follows that $\Gamma=M_l x$.

Equation (4) can now be differentiated with respect to x and substituted into equation (6). After rearranging this gives

$$h'''=\left(1+(h')^2\right)^{2/3}\left(\frac{b}{h^3}+ah'+\frac{3h'(h'')^2}{\left(1+(h')^2\right)^{5/2}}\right) \tag{7}$$

with

$$a=\frac{\rho_l g}{\sigma}$$

$$b=\frac{3\mu_l\Gamma}{\sigma\rho_l}$$

The boundary conditions for equation (7) are discussed in detail in section (c) below.

Ignoring the surface tension term in equation (4) and following a similar procedure as in the derivation of equation (7) it follows that

$$h=-\frac{3\mu_l\Gamma}{\rho_l^2 g h^3} \tag{8}$$

Integrating equation (8) with $h_{W/2}=0$ (see Bejan [2]) yields the following relation, which describes the profile of the dynamic meniscus in the absence of surface tension:

$$h=\left(\frac{12\mu_l\Gamma}{\rho_l^2 g}\left(\frac{W}{2}-x\right)\right)^{1/4} \tag{9}$$

(b) Static solution ($\Gamma=0$)

From the force balance in a static liquid film it follows that

$$\frac{dP}{dy}=-\rho_l g \tag{10}$$

At the free surface of the static meniscus equation (4) can be rewritten as

$$P=P_{atm}-\frac{\sigma h''}{\left(1+(h')^2\right)^{3/2}} \tag{11}$$

Integrating equation (10) from $y=0$ to $y=h$ and substituting equation (11) into the resulting equation together with the boundary conditions $h=h_{sc}$ and $h'=0$ at $x=0$ yields

$$-\frac{h''}{\left(1+(h')^2\right)^{3/2}}=\frac{\rho_l g}{\sigma}(h_{sc}-h)-h''_{sc} \tag{12}$$

Integrating equation (12) between $x=0$ and $x=(W/2)$ yields

$$h'=-\frac{\left(1-\left(1-\frac{\rho_l g}{2\sigma}(h-h_{sc})^2-h''_{sc}(h-h_{sc})\right)^2\right)^{1/2}}{1-\frac{\rho_l g}{2\sigma}(h-h_{sc})^2-h''_{sc}(h-h_{sc})} \tag{13}$$

which with boundary conditions

$h'_s=\tan\theta$ at $x=\frac{W}{2}$

and

$h_s=0$ at $x=\frac{W}{2}$

can be used to determine the static liquid surface profile.

From equation (13) and its boundary conditions it follows that

$$h_{sc}=\frac{\sigma h''_{sc}}{\rho_l g}+\left(\left(\frac{\sigma h''_{sc}}{\rho_l g}\right)^2+\frac{2\sigma(1-\cos\theta)}{\rho_l g}\right)^{1/2} \tag{14}$$

Equations (13) and (14) reduce to the corresponding relations given by Ishimi *et al.* [9] if $h''_{sc} = 0$ (see equation 1).

(c) Sample solutions

Static meniscus ($\Gamma = 0$)

Figure 2 shows a meniscus formed at a sharp edged slat. The Gibbs equation (Gibbs [11]) gives the critical angle for liquid spreading over a sharp edge of a solid as

$$\theta_c = (180° - \phi) + \theta_c \qquad (15)$$

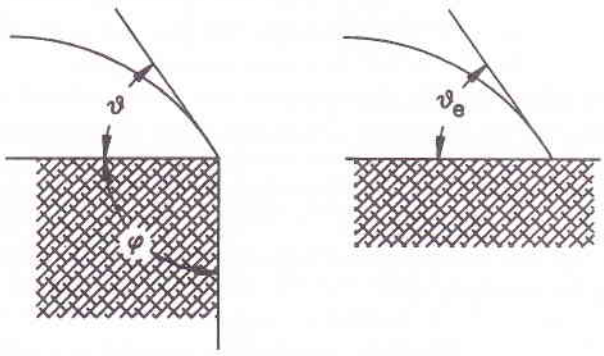


Figure 2 Definitions of the angles at edges and on horizontal surfaces

The height of the meniscus in the centre of the slat is a maximum when $\theta = \theta_c$. The equilibrium (thermodynamic) contact angle or the so-called wetting angle, θ_e, is zero for liquid that wets the solid perfectly. In the case of non-perfect wetting the wetting angle will be larger than 0°. For a perfectly wetting liquid on a sharp edge with $\phi = 90°$, equation (15) predicts a critical angle of 90°. This was confirmed experimentally by Oliver *et al.* [12] and Bayramli & Mason [13] for very sharp edges. Oliver *et al.* found that the static liquid film becomes unstable when θ_c approaches 180° or when the contact line has advanced passed the edge, resulting in liquid flowing over the edge due to gravity.

The static solution of a liquid meniscus, with a known value of θ, on a narrow slat of width, W, can be found as follows:

1. assume a value for h_{sc},
2. assume a value for h''_{sc}
3. integrate equation (7) with $b = 0$ (since $\Gamma = 0$ for the static solution) numerically from $x = 0$ to $x = (W/2)$,
4. if $h_{W/2} \approx 0$ the value of h_{sc} assumed in step 2. was correct, else repeat from step 2.,
5. calculate h_{sc} from equation (14),
6. repeat from step 1. until h_{sc} converges.

For water on a slat with square edges ($\phi = \theta_c = 90°$), Figures 3, 4, and 5 show the results of the calculation procedure described above. Figure 6 shows the ratio between the pressure due to surface tension and the hydrostatic pressure over the width of the slat. This ratio strongly influences the shape of the meniscus. It can be noted that for the narrow slats ($W = 5$ mm and $W = 10$ mm) the surface tension term dominates the hydrostatic pressures while the surface tension term becomes relatively small in the middle regions of the wider slats.

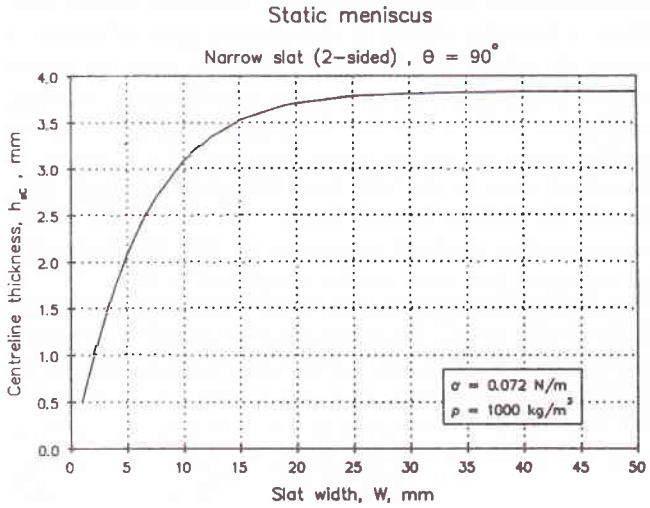


Figure 3 Predicted static centreline film thicknesses on narrow slats

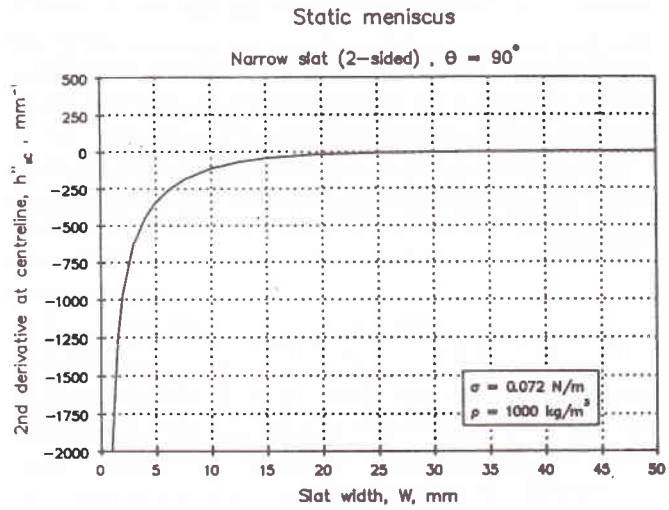


Figure 4 Predicted variation of the h''_{sc} on narrow slats. Note that $h''_{sc} \to 0$ as the slat width increases

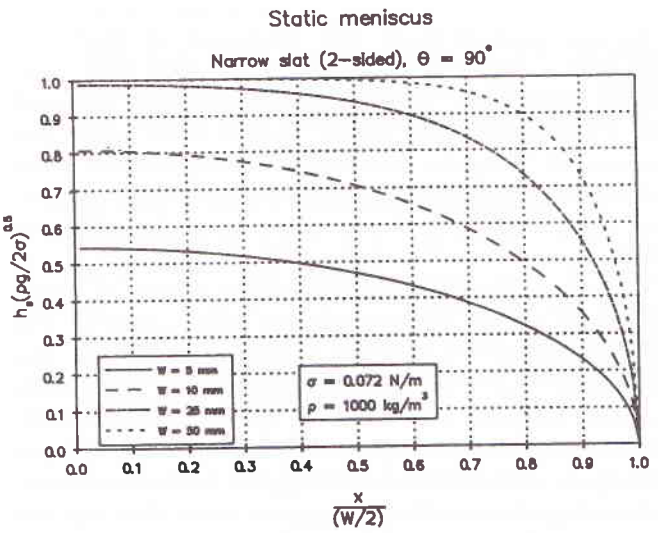


Figure 5 Predicted film profiles for static meniscii on different slats

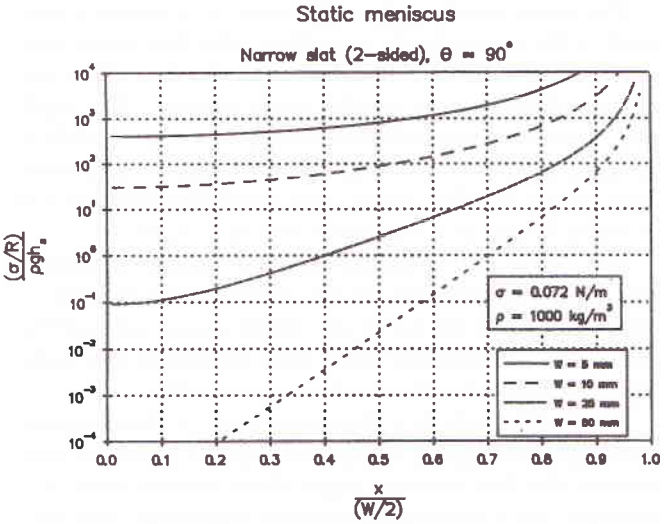


Figure 6 Ratio between pressure die to surface tension and hydrostatic pressure along the width of a narrow slat

Meniscus for non-zero liquid flow rate ($\Gamma > 0$)

The differential equation governing the flow of liquid over the edge of a horizontal slat is of the third order, implying that three boundary conditions are required to solve this equation.

On a very wide slat it is known that h' and h'' far from the edge will be zero. In the centre of a narrow slat, h' will be zero but h'' will not equal zero. For the case of a narrow slat, only the first boundary condition is certain and approximate methods have to be employed to find the other two boundary conditions.

Model A

It is expected that $0° > \theta > \theta_c$. For very low flow rates it can be assumed that $\theta \approx \theta_c$ and $h_{W/2} \approx 0$. In this case the solution of the equation (7) proceeds as follows:

1. assume h_{dc}
2. assume h''_{dc}
3. integrate equation (7) numerically from $x = 0$ to $x = (W/2)$
4. if $h'_{W/2} \neq -\tan\theta_c$ repeat from step 2.
5. if $h_{W/2} \neq 0$ then repeat from step 1.

Model B

Alternatively, following the modelling approach of Ishimi *et al.*,[9] the meniscus at a non-zero liquid flow rate can be assumed to be similar to the static meniscus which implies that $h''_{sc} \approx h''_{dc}$. The equation by Ishimi *et al.*, equation (2), can be used to approximate h_{dc}. In this case the solution of the equation (7) proceeds as follows:

1. find h_{sc}, as described above
2. calculate h_{dc}, from equation (2)
3. set $h''_{sc} = h''_{dc}$
4. integrate equation (7) numerically from $x = 0$ to $x = (W/2)$

Model C

A third method to solve equation (7) would involve measuring the value of h_{dc} experimentally and then using this value together with $h_{w/2} = 0$ (or alternatively with $h'_{W/2} = -\tan\theta$).

Figure 7 compares the solutions obtained with models A and B for slat widths of 10 and 25 mm with $\phi = 90°$. Note that in the case of the Model A solutions it was assumed that $h'_{W/2} = -\tan(89°)$ instead of $h'_{W/2} = -\tan(90°)$ due to numerical difficulties at $x = (W/2)$ if $\theta = 90°$. Using an arc-length formulation to describe the curvature term in equation (4) could avoid this numerical difficulty, but from the experimental work which follows it can be seen that an angle of $0 = 90°$ at $x = (W/2)$ is an extreme value and that the actual angle is expected to be less than 90°.

Figure 8 compares the prediction of Model B for the cases when $\Gamma(x) = C$ i.e. with liquid supplied centrally and when $\Gamma(x) = M_1 x$, with liquid supply evenly distributed over the slat width. The value of M_1 was

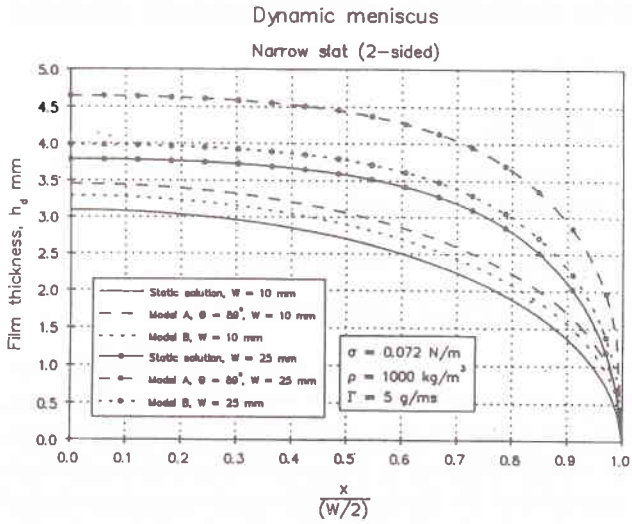


Figure 7 Comparison between predicted static and dynamic film profiles

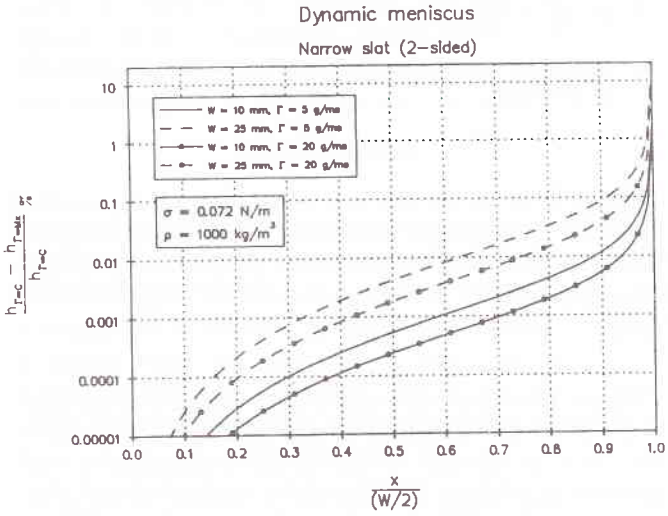


Figure 8 Differences in film thickness with the liquid supplied centrally and with an evenly distributed supply to the slat

selected to yield the same mass flow rate per unit length at $x = (W/2)$, i.e. $M_l = C/(W/2)$. From Figure 8 it can be seen that for a range of flow rates the differences in the film thicknesses determined for these two cases are very small (except right on the edge).

Experimental study

An experimental study was conducted in which the meniscus profiles of liquid on narrow slats were measured. In all tests, water at room temperature was used as a test liquid. The surface tension of the water was measured (using the drop weight method) several times during the experiments and this confirmed that the water surface tension was very close to that of distilled water.

The experimental setup consisted of a frame on which a supply trough and the test slat were mounted. The frame allowed for accurate adjusting of the test slat to ensure that it was perfectly horizontal. The supply trough consisted of a 25 mm × 25 mm × 300 mm aluminium bar with a 2 mm × 200 mm slot machined into its upper surface. Water was supplied to slot in the supply trough from a 10 mm diameter tube. The test slat was secured to the top of the supply trough. To ensure an even water supply to the upper surface of the slats, each test slat had a number of small holes drilled through it (to allow the flow of water from the water supply slot) on the centreline.

The water supply system consisted of a constant head tank (with an overflow), a capillary tube flow meter with a water manometer, and a fine control valve. This system produced a very steady water supply. The capillary flow meter was calibrated using an accurate scale to measure mass flow rate over given periods. The pressure drop across the flow meter was approximately 600 mm of water height at a mass flow rate of 1.3 g/s.

The height of the liquid film was measured using a dial type vernier height gauge. It was relatively easy to determine when the tip of the height gauge touched the water film, since small waves were formed on the water film which could easily be observed visually.

At the relatively low flow rates used in these experiments ($\Gamma < 2.5$ g/ms) it was not possible to ensure continuous film flow over the edges of non-wetting slats. For example, for a thoroughly cleaned aluminium slat with square edges, $\phi = 90°$, the equilibrium contact angle (i.e θ_e) was significantly larger than 0°, which implies a critical contact angle greater than 90° according to the Gibbs relation (equation 15). The following sequence of events was observed for an aluminium slat supplied with a constant water flow rate. Initially the water film on an aluminium slat would grow in height until the critical contact angle, θ_c, was reached, at which point the water pours over the edge. The liquid film thickness decreases significantly until a point where the liquid flow over the edge ceases. The film then starts to grow again and the process described above is repeated. In some cases this cycling motion was not observed and one or more small rivulets would form at certain positions along the slat

through which the liquid would flow over the edge. In this case the liquid height would remain fairly constant. For a 25 mm wide aluminium slat with only one rivulet (at the end of the slat) the centreline film height was found to agree closely to the predicted static meniscus height with $\theta_s = 90°$.

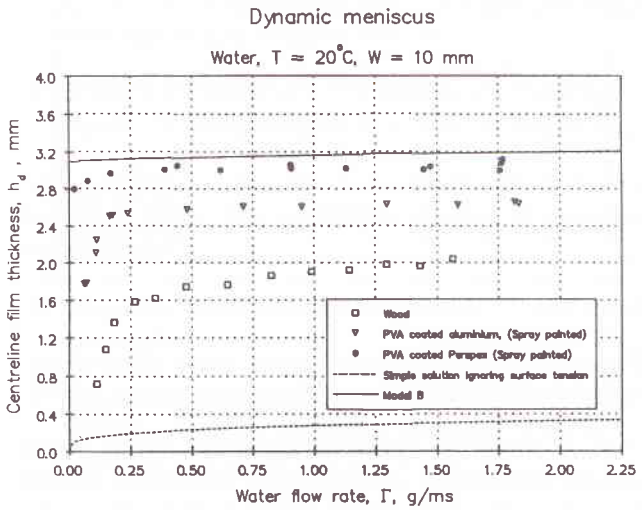


Figure 9 Experimentally determined centreline film thicknesses on various 10 mm wide slats compared to theoretical predictions

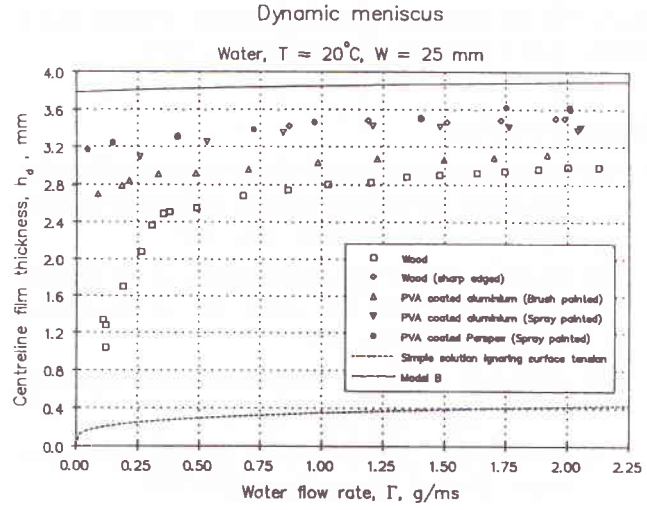


Figure 10 Experimentally determined centreline film thicknesses on various 25 mm wide slats compared to theoretical predictions

Various types of slats were used. Wooden slats gave very even wetting, but it was difficult to produce very sharp edges consistently. Even if the wooden slats had very sharp edges in the dry state, this was not necessarily the case when they were wet. The film thicknesses measured on the wooden slats also tended to vary with time due to the wood absorbing water. It was also observed that aluminium slats coated with common PVA (polyvinyl alcohol) paint would wet evenly with a very small contact angle. It was found that PVA paint held well on sandblasted Perspex. It was possible to obtain sharper edges with the PVA coated Perspex slats than with the PVA coated aluminium slats.

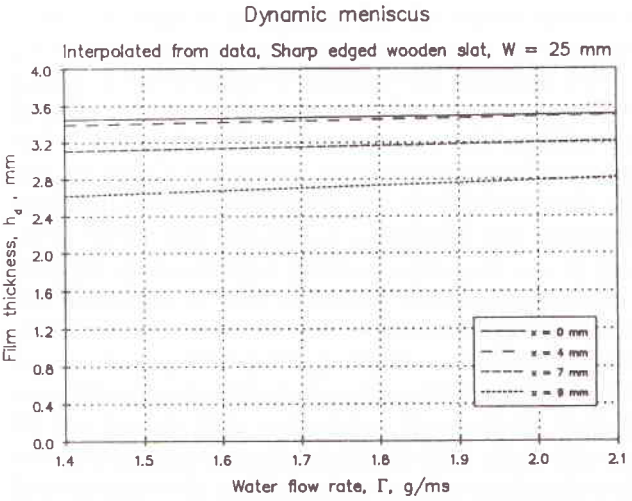


Figure 11 Experimentally determined variation of film profile with liquid flow rate on a 25 mm wide sharp-edged wooden slat

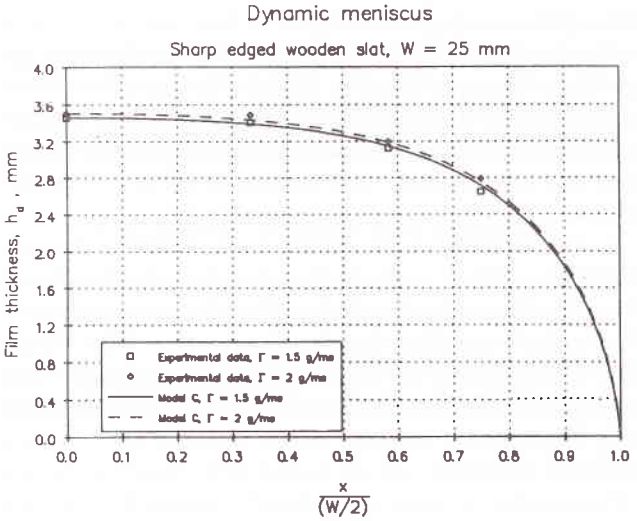


Figure 12 Correlation between measured and calculated film profiles on a 25 mm wide sharp-edged wooden slat

Figures 9 and 10 give typical centreline film thicknesses measured on the 10 and 25 mm wide slats for various water flow rates. It can be noted from some of the data that the centreline film thickness falls sharply

as the water flow rate is reduced. This is thought to be due to imperfections on edges which result in no static meniscus being formed. Generally, it was observed that the water films were thicker on slats with sharper edges.

Figures 11 and 12 show measured film thicknesses at other positions along the width of a slat. it was not possible to measure the film thicknesses closer to the edge of the slat due to the high gradient near the edge.

Discussion

When using water as the liquid on the slat, the effect of slat width on the static centreline film thickness is less important for slats wider than 20 mm (see Figure 3). For slats narrower than 20 mm, the maximum film thickness (centreline film thickness) is reduced due to the proximity of the two edges and the corresponding increase in the influence of the curvature term in equation (11). The effect of slat width on the centreline film thickness is expected to be similar for low liquid flow rates.

Figures 9 and 10 show the prediction of simple solution and that of Model B (with $\theta_s = 90°$) for 10 and 25 mm wide slats. The simple solution, which ignores the effect of surface tension underpredicts the experimental data by far, and it also fails to predict a static meniscus. Model B, on the other hand, overpredicts the centreline film thicknesses, probably due to the assumption of a static contact angle of $\theta_s = 90°$. The predicted and the measured centreline film thicknesses increase at a similar rate with increasing flow rate.

The agreement between the measured profiles in Figure 12 and that predicted by Model C is very good. Note that in Model C the experimentally determined centreline film thickness is used as one of the boundary conditions and consequently this data point (at $x = 0$) corresponds exactly to the predicted profile.

It was possible to use Model C to calculate the approximate contact angle at the edge, θ, using the experimentally determined centreline film thicknesses. Figure 13 shows the results of such calculations. This figure shows that the contact angle at the edge increases with increasing flow rate and that it tends to flatten off at the high flow rates.

Conclusions

The effect of surface tension is of utmost importance in determining the free surface profile and film thickness for low flow rate flow over sharp edged horizontal surfaces. Surface wetting, edge radii and slat widths also play important roles in governing the free surface profile on a slat.

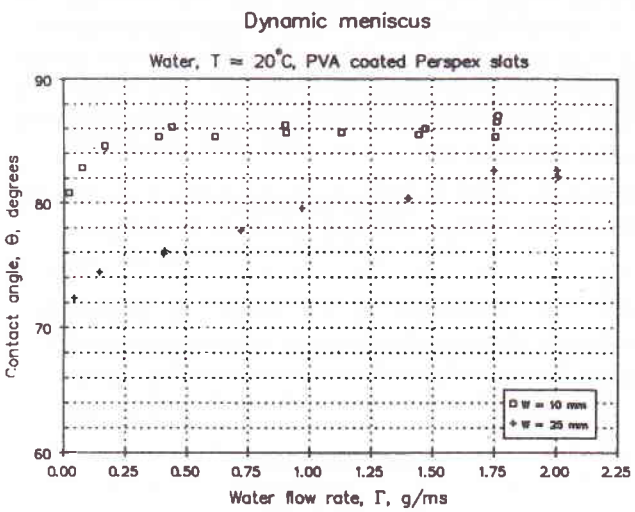


Figure 13 Calculated contact angles at the edges of the 10 mm and 25 mm wide PVA coated Perspex slats

The approximate mathematical model using experimentally determined centreline film thicknesses (Model C) predicts the free surface profile well for flow rates below 2.5 g/ms.

Model B, with θ_s slightly less than 90° (say $\theta_s = 89°$), can be used to predict the profile of a liquid film on a sharp-edged slat ($\phi = 90°$). This model, with $\theta_s = 90°$, is expected to represent the asymptotic film thickness which will be achieved with a perfectly wetting liquid flowing over a perfectly sharp edge ($\phi = 90°$).

References

[1] Leppert G & Nimmo B 1968. Laminar film condensation on surfaces normal to body or inertial forces. *J. Heat Transfer*, 178–179.

[2] Bejan A 1991. Film condensation on an upward facing plate with free edges. *Int. J. Heat Mass Transfer*, **34**, 578–582.

[3] Probstein RF 1989. *Physicochemical Hydrodynamics.* Butterworths, Boston.

[4] Slocum EW 1964. Flow of viscous fluids over weirs. *Can. J. Chem. Eng.*, 196–200.

[5] Nedderman RM 1966. The flow of thin films down nearly horizontal surfaces. *Chem. Eng. Sci.*, **21**, 715–717.

[6] Goodridge F & Gartside G 1965. Mass transfer into near-horizontal liquid films. Part 1. Hydrodynamic studies. *Trans. Inst. Chem. Eng.*, **43**, T62–T67.

[7] Nimmo B 1972. Thin film flow on curved surfaces. *Chem. Eng. Sci.*, **27**, 695–701.

[8] Bergink-Martens DJM, Bos HJ, Prins A & Schulte BC 1990. Surface dilation and fluid-dynamical behaviour of Newtonian liquids in an overflowing cylinder. 1. Pure liquids. *J. Colloid Interface Sci.*, **138**, 1–9.

[9] Ishimi K, Koroyasu S & Hikita H 1986. Flow of liquids in the entrance region of wetted-wall columns with an overflow-type distributor. *Bull. Univ. Osaka Pref, Series A. Eng. and Nat. Sci.*, **35**, 75–83.

[10] Hartland S & Hartley RW 1976. *Axisymmetric fluid-liquid interfaces*. Elsevier Scientific Publishing Company, Amsterdam.

[11] Gibbs JW 1976. *Scientific Papers*, **1**, **326**, 1906. (referred to by Bayramli & Mason, 1978).

[12] Oliver JF, Huh C & Mason SG 1977. Resistance to spreading of liquids by sharp edges. *J. Colloid Interface Sci.*, **59**, 568–581.

[13] Bayramli E & Mason SG 1978. Liquid spreading: Edge effect for zero contact angle. *J. Colloid Interface Sci.*, **66**, 200–202.